Extra-Low-Temperature Oxygen Storage Capacity of CeO2 Nanocrystals with Cubic Facets

ARTICLE *in* NANO LETTERS · JANUARY 2011

Impact Factor: 13.59 · DOI: 10.1021/nl102738n · Source: PubMed

10 AUTHORS, INCLUDING:

Akira Morikawa
Toyota Central R & D Labs., Inc.
12 PUBLICATIONS **223** CITATIONS
SEE PROFILE

Hirofumi Shinjoh
Toyota Central R & D Labs., Inc.
80 PUBLICATIONS **2,288** CITATIONS
SEE PROFILE

Kenji Kaneko
Kyushu University
235 PUBLICATIONS **4,316** CITATIONS
SEE PROFILE

Akihiko Suda
Toyota Central R & D Labs., Inc.
11 PUBLICATIONS **198** CITATIONS
SEE PROFILE

NANO LETTERS

LETTER

pubs.acs.org/NanoLett

Extra-Low-Temperature Oxygen Storage Capacity of CeO_2 Nanocrystals with Cubic Facets

Jing Zhang,[⊥,†] Hitoshi Kumagai,[‡] Kae Yamamura,[‡] Satoshi Ohara,[#,†] Seiichi Takami,[†] Akira Morikawa,[‡] Hirofumi Shinjoh,[‡] Kenji Kaneko,[§] Tadafumi Adschiri,[*,†,∥] and Akihiko Suda[*,‡]

[†]Institute of Multidisciplinary Research for Advanced Materials (IMRAM), Tohoku University, 2-1-1, Katahira, Aoba-ku, Sendai 980-8577, Japan

[‡]Catalyst Lab., Sustainable Mater. Div., Toyota Central Research & Development Laboratories, Inc., 41-1, Nagakute, Aichi 480-1192, Japan

[§]Department of Material Science and Engineering, Kyushu University, 744, Motooka, Nishi-ku, Fukuoka 819-0395, Japan

[∥]Advanced Institute for Materials Research (AIMR), Tohoku University, Japan

Supporting Information

ABSTRACT: Herein we demonstrate the extra-low-temperature oxygen storage capacity (OSC) of cerium oxide nanocrystals with cubic (100) facets. A considerable OSC occurs at 150 °C without active species loading. This temperature is 250 °C lower than that of irregularly shaped cerium oxide. This result indicates that cubic (100) facets of cerium oxide have the characteristics to be a superior low-temperature catalyst.

KEYWORDS: Cerium oxide, nanocrystals, cubic facets, oxygen storage capacity, catalyst

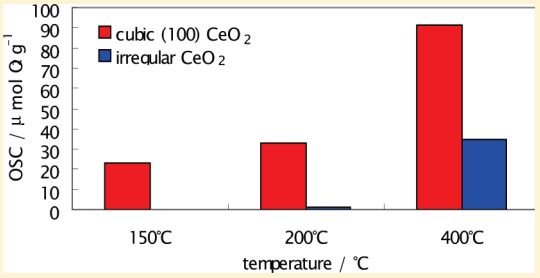

Cerium oxide has received much attention due to its ability as a three-way catalyst in the exhaust system of automobiles[1,2] and as primary oxygen storage material.[2,3] Because the catalytic activity of cerium oxide originates from the surface oxygen,[4] the active oxygen content at the cerium oxide surface must be increased to improve catalytic activities. Cerium oxide is a highly stable fluorite structure and a one-electron redox agent. The effective ionic radii of Ce^{4+} and O^{2-} are 0.10 and 0.14 nm, respectively;[5] the relative ionic radius of Ce^{4+}/O^{2-} is 0.71, resulting in a coordination number of cerium to oxygen atoms of 8 and that of oxygen to cerium atoms of 4. This 8 to 4 coordination permits oxide defects in $CeO_{(2-X)}$ over a wide range of X values, which approach 0.5.[6] Previous experimental and theoretical studies have shown that increasing the specific surface area can optimize the catalytic activity of cerium oxide.[7]

Recently, an alternative strategy to enhance the oxygen storage capacity (OSC) of cerium oxide has been introduced by modifying the morphology of cerium oxide.[8−10] In particular, the (100) facet of cerium oxide is the best catalytic candidate for highly reactive surfaces.[8] The six (100) planes have the highest surface energy among the low-index crystal planes. This high surface energy originates from the instability of the top-layer oxygen, which is located at the bridging positions between two cerium ions.[11]

Herein, we propose a modified approach to fabricate cerium oxide nanocrystals with a controlled size of about 10 nm that is morphologically bound by six (100) planes via an organic-ligand-assisted supercritical hydrothermal process.[12,13] Interestingly, cerium oxide nanocrystals with six (100) facets show an enhanced OSC performance at lower temperature compared to those with irregular morphologies. The extra-low-temperature OSC of the cerium oxide nanocrystals with cubic (100) facets described herein opens a route for low-temperature industrial applications such as innovative exhaust catalysts.

Cerium oxide nanocrystals with cubic (100) facets were prepared by a modified hydrothermal synthesis.[12,13] The cerium oxide precursor was precipitated from 0.1 M of a cerium(III) nitrate aqueous solution by adding 25% ammonia aqueous solution in a 100 mL glass beaker while stirring with a magnetic stirrer. The freshly prepared cerium oxide precursor with water (2.5 mL, 0.02 M−Ce) and hexanoic acid (0.2 mL) was transferred into a pressure-resistant SUS316 vessel (inner volume, 5 mL). The supercritical hydrothermal synthesis was carried out in the reaction vessel at 400 °C for 10 min. The reaction vessel was then allowed to cool in a water bath. The aggregated nanocrystals were filtered, subsequently washed with water and ethanol, and then dried in air. A comparable sample of irregularly shaped cerium oxide powder was also prepared by calcination of the cerium oxide precursor at 400 °C for 10 min.

The samples were analyzed using a Nicolet AVATAR 360 FT-IR spectrometer to measure the infrared (IR) spectra, a Hitachi

Received: August 4, 2010
Revised: December 11, 2010

dx.doi.org/10.1021/nl102738n | *Nano Lett.* XXXX, XXX, 000–000

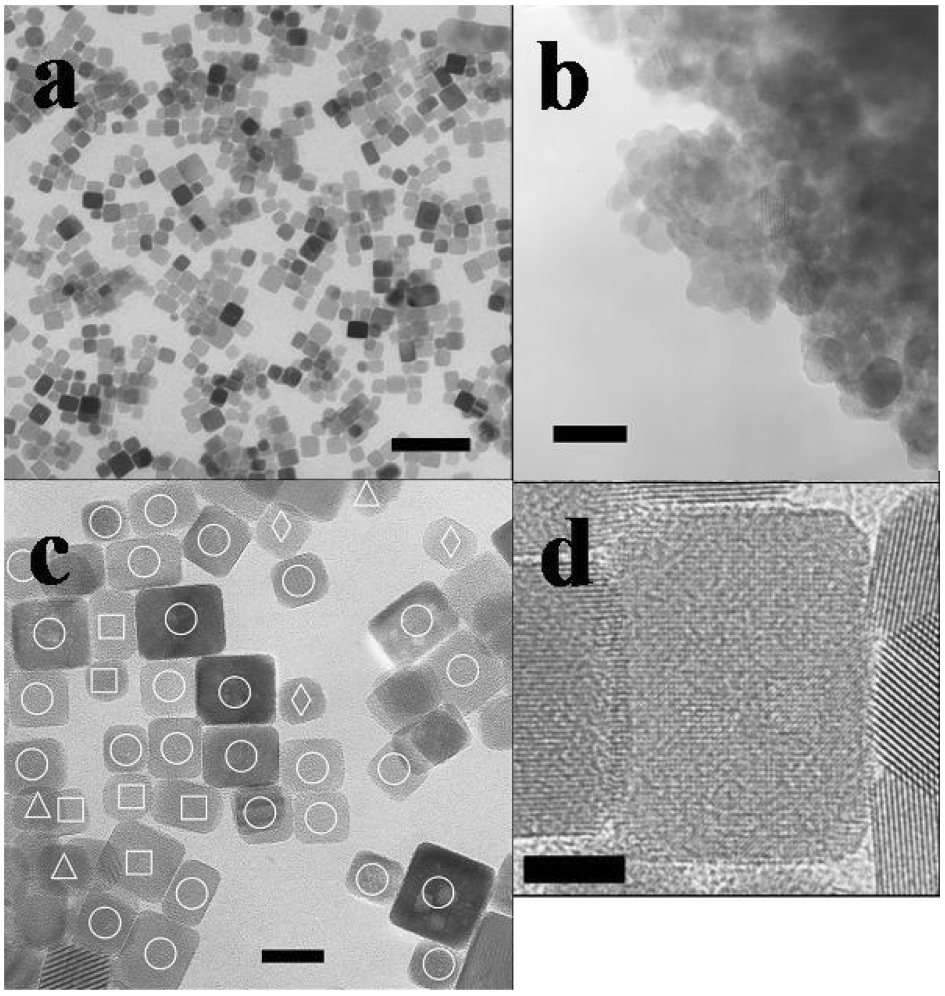

Figure 1. (a) TEM image of cerium oxide nanocrystals with cubic (100) facets. Scale bar, 50 nm. (b) TEM image of an irregular shape cerium oxide powder. Scale bar, 20 nm. (c) TEM image of cerium oxide nanocrystals with cubic (100) facets with group markings. Circles correspond to the first group with a {200} waffle pattern. Squares correspond to the second group with {200}{220} lattice fringe. Diamonds correspond to the third group with {110} lattice fringe. Triangles correspond to the fourth group with {111} lattice fringe. Scale bar, 10 nm. (d) High-resolution TEM image of cubic cerium oxide nanocrystals. Scale bar, 5 nm.

H-9000UHR for conventional TEM observations, and FEI TECNAI-20 for three-dimensional TEM observations. Thermogravimetric (TG) analysis was carried out by a Shimadzu TGA-50 from room temperature to 400 °C under a 20% O_2 (N_2-balanced) atmosphere, and then the OSC was calculated from the weight loss and gain after several cycles of reduction and oxidation. Cerium oxide nanocrystals with (100) facets were initially treated at 150 °C for 1 h in air to remove hexanoic acid from the surface. The sample was oxidized in 20% O_2 (N_2-balanced) and then reduced in 12% H_2 (N_2-balanced) and oxidized repeatedly at 150, 200, and 400 °C. (See Figure S1, Supporting Information.) The BET surface area was measured on a Micro Data automatic surface area analyzer model 4232.

Regardless of the synthetic method (supercritical hydrothermal process or calcinations), the X-ray diffraction patterns of both samples correspond to the cubic fluorite structure of CeO_2 (Figure S2, Supporting Information). Figure S3 (Supporting Information) shows the IR spectra of the hydrothermally synthesized sample before and after TG measurements. The IR spectrum prior to the TG measurements has strong absorption bands in the 2800−3000 cm^{-1} regions, which are attributed to the C−H stretching mode of the methyl and methylene groups. The other bands at 1530 and 1540 cm^{-1} originate from the stretching frequencies of the carboxylate group. The presence of these bands indicates bonding between the organic ligand molecules and the surface of the nanocrystals, which leads to the formation of cerium oxide nanocrystals with cubic (100) facets. This structural feature is very similar to the cerium oxide nanocrystals prepared with decanoic acid.[12] An abrupt weight loss is observed around 150 °C in the TG trace of the as-prepared hydrothermally synthesized sample (Figure S4, Supporting Information). Additionally, the characteristic absorption bands are absent in the IR spectrum from the sample after the TG measurements. Thus, the weight loss of the sample is simply due to the loss of an organic moiety from the crystal surface.

Panels a and b of Figure 1 show the conventional TEM images of cerium oxide nanocrystals prepared by supercritical hydrothermal synthesis with hexanoic acid and by calcination of the cerium oxide precursor, respectively. As shown in Figure 1a, the cerium oxide crystals prepared by supercritical hydrothermal synthesis exhibit a highly dispersed square shape with an average size of about 10 nm, whereas the cerium oxide powder prepared

dx.doi.org/10.1021/nl102738n |*Nano Lett.* XXXX, *XXX*, 000–000

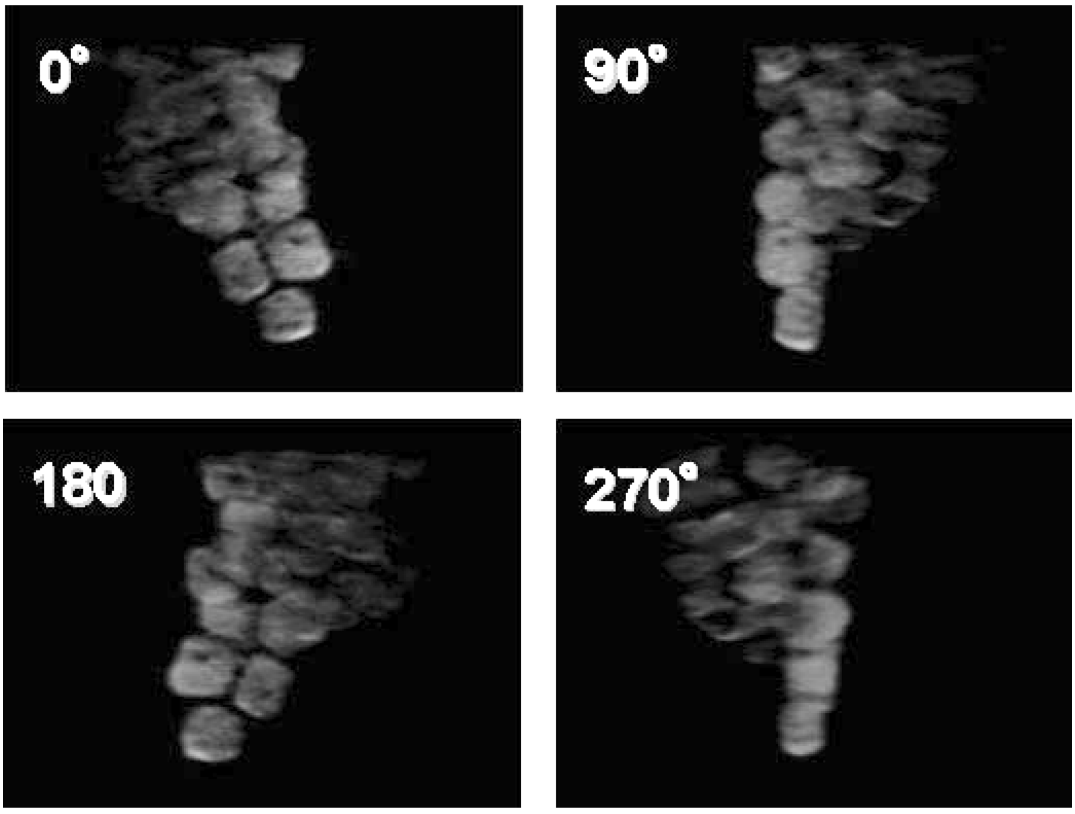

Figure 2. 3D TEM images corresponding to the clockwise rotation of the structure at 0°, 90°, 180°, and 270° of an aggregated powder of cerium oxide nanocrystals with cubic (100) facets.

by calcination consists of aggregated crystallites with irregular morphologies. The particle sizes of irregular cerium oxide nanoparticles were about 10 nm, which is consistent with the average crystallite size calculated from the XRD peaks using the Scherrer equation. Figure 1c is a high-magnification micrograph of hydrothermally synthesized particles. Figure S5 (Supporting Information) shows the electron beam diffraction pattern corresponding to the area of Figure 1c. The electron beam diffraction pattern reveals that all the detectable reflections are indexed to the same positions as those of the cubic fluorite structure of CeO_2, and the {200} diffraction has a relatively high intensity.

The individual cerium oxide nanocrystals can be classified into four groups by reverse-Fourier transformation of the lattice image of each cerium oxide nanocrystal lined up on the carbon film grid of TEM (Figure S6, Supporting Information). Nearly 70% of the crystals (marked by circles) are classified as the first group with {200}, which corresponds to cerium oxide nanocrystals with cubic (100) facets. Figure 1d shows a magnified image in which the waffle pattern can be observed. Fifteen percent of the crystals can be classified as the second group (denoted by squares in Figure 1c), which shows a {200} {220} lattice fringe. Although the second group also displays {200} lattice fringes, orthogonal stripes could not be observed, which may be because the second group is inclined to the carbon film grid of the TEM. It is highly likely that the second group is cerium oxide nanocrystals with cubic (100) facets. The remaining crystals are evenly divided between the third (denoted by diamonds) and fourth (denoted by triangles) groups, which show {110} lattice fringes and {111} lattice fringes, respectively. Therefore, it is considered that the ceria nanocrystals prepared by supercritical hydrothermal synthesis may have two kinds of shape; main nanocrystals are cube and/or slightly truncated cube[13] and the remaining other smaller ones are truncated octahedron. Furthermore, we successfully produced a three-dimensional reconstructed image of the cerium oxide nanocrystals with {200}. Figure 2 shows four still photographs; each 3D image corresponds to the clockwise rotation of the structure at 0°, 90°, 180°, and 270°. These images support the assertion that cerium oxide nanocrystals have cubic morphologies with (100) facets and not a thin plate shape.

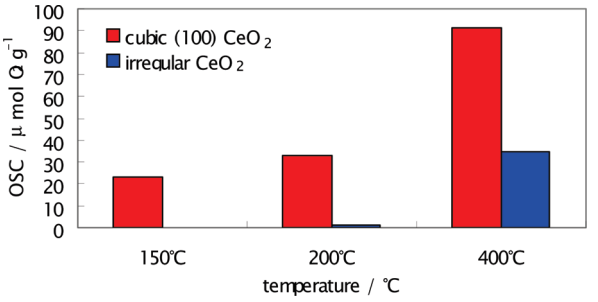

Figure 3. Comparative OSC of cerium oxide nanocrystals with cubic (100) facets and a sample of irregularly shaped cerium oxide powder.

Figure 3 compares the OSC of the two different types of cerium oxide nanocrystals, the one with cubic (100) facets and the other with an irregular morphology, at different temperatures. The BET surface areas of cubic and irregular cerium oxide nanocrystals are 61 and 100 m^2/g, respectively. Two differences are identified. Although the cubic nanocrystals have a smaller

dx.doi.org/10.1021/nl102738n |*Nano Lett.* XXXX, *XXX*, 000–000

surface area than the irregular particles, the OSC of cerium oxide nanocrystals with cubic (100) facets is nearly 2.6 times higher at 400 °C. Additionally, the effective activating temperature of OSC is 150 °C for the cerium oxide nanocrystals with cubic (100) facets, but 400 °C for the irregular morphologies with a low OSC.

The BET surface area of cerium oxide nanocrystals with cubic (100) facets is 61 m^2/g, whereas the calculated surface area for 1 g of 10 nm cubic CeO_2 crystallites is 137.0 m^2/g. The calculated and the measured values seem to be consistent, considering the aggregation level of each crystallite observed in Figures 1a, 1c, and 2. Highly dispersed and ordered particles could easily result in a strong aggregation, which reduces the effective BET surface area. Assuming that two of the four oxygen sites are involved in the OSC process, the estimated[11] number of the surface oxygen atoms is 5.7 μmol of O_2/m^2. Hence, the theoretical OSC is calculated to be 357 μmol of O_2/g for 61 m^2/g.

There are two reasons that the theoretical OSC is much higher than the measured value in Figure 3. First, the activation energy is insufficient for the remaining oxygen to be released, particularly at 150 and 200 °C. Second, the cerium oxide nanocrystals can degrade at 400 °C; the cerium oxide nanocrystals with cubic (100) facets do not maintain their cubic morphology after 5 h of reduction and oxidation treatments at 400 °C (Figure S7, Supporting Information). Hence, lanthanum ions were introduced into the nanocrystals to improve the thermal stability of the cerium oxide nanocrystals with cubic (100) facets. Figure S8 (Supporting Information) shows TEM images of lanthanum-containing cerium oxide nanocrystals; these crystals form similar nanocrystals with cubic morphologies. Further characterization of La-containing cerium oxide nanocrystals is in progress.

In summary, single-crystalline cerium oxide nanocrystals with dimensions of about 10 nm with (100) facets were synthesized via organic ligand-assisted supercritical hydrothermal syntheses. The extra-low-temperature OSC performance was confirmed in cerium oxide nanocrystals with cubic (100) facets by comparing the OSC performance of the cubic nanocrystals to that of the irregularly shaped cerium oxide. We expect that this work will aid in the development of a shape-controlled synthetic methodology for inorganic nanocrystals. Furthermore, these cubic nanocrystals show promise in the design of catalytic materials with higher performances by controlling the formation of well-defined crystal planes.

■ ASSOCIATED CONTENT

Supporting Information. Figures of TG analysis for OSC, X-ray diffraction patterns, IR spectra, an electron beam diffraction pattern, and TEM images. This material is available free of charge via the Internet at http://pubs.acs.org.

■ AUTHOR INFORMATION

Corresponding Author

*E-mail address: ajiri@tagen.tohoku.ac.jp (T.A.); a-suda@mosk.tytlabs.co.jp (A.S.).

Present Addresses

[⊥]Chinese Academy of Science, China.

[#]Joining and Welding Research Institute, Osaka University, Japan.

■ ACKNOWLEDGMENT

We thank T. Nakayama and K. Niihara of Nagaoka University of Technology for showing us the future prospects of this research on the crystal face control of ceria.

■ REFERENCES

(1) Kummer, J. T. *Proc. Energy Combust. Sci.* **1980,** *6*, 177.
(2) Yao, H. C.; Yao, Y. F. Yu *J. Catal.* **1984,** *86*, 254–265.
(3) Di Monte, R.; Kasper, J.; Bradshaw, H.; Norman, C. *J. Rare Earth* **2008,** *26*, 136–140.
(4) Tanabe, T.; et al. *Stud. Surf. Sci. Catal.* **2001,** *138*, 135–144.
(5) Shannon, R. D.; Prewitt, C. T. *Acta Crystallogr., Sect. B* **1969,** *25*, 925–946.
(6) Wu, L. J.; et al. *Phys. Rev. B* **2004,** *69*, No. 125415.
(7) Masui, T.; Fujiwara, K.; Machida, K.; Adachi, G. *Chem. Mater.* **1997,** *9*, 2197–2204.
(8) Skorodumova, N. V.; Baudin, M.; Hermansson, K. *Phys. Rev. B* **2004,** *69*, No. 075401.
(9) Mai, H. X.; Sun, L.-D.; Zhang, Y.-W.; Si, R.; Feng, W.; Zhang, H.-P.; Liu, H.-C.; Yan, C.-H. *J. Phys. Chem. B* **2005,** *109*, 24380–24385.
(10) Zhou, K.; et al. *J. Catal.* **2005,** *229*, 206–212.
(11) Norenberg, H.; Harding, J. H. *Surf. Sci.* **2001,** *477*, 17–24.
(12) Zhang, J.; et al. *Adv. Mater.* **2007,** *19*, 203–206.
(13) Kaneko, K.; Inoke, K.; Freitag, B.; Hungria, A. B.; Midgley, P. A.; Hansen, T. W.; Zhang, J.; Ohara, S.; Adschiri, T. *Nano Lett.* **2007,** *7*, 421–425.